# A Generic Approach to the Theory of Superregenerative Reception

F. Xavier Moncunill-Geniz, Pere Palà-Schönwälder, *Member, IEEE*, and Orestes Mas-Casals

***Abstract*—The superregenerative receiver has been widely used for many decades in short-range wireless communications because of its relative simplicity, reduced cost, and low power consumption. However, the theory that describes the behavior of this type of receiver, which was mainly developed prior to 1950, is of limited scope, since it applies to particular implementations, usually operating under continuous-wave signal or narrow-band modulation. As a novelty, we present the theory of superregenerative reception from a generic point of view. We develop an analytic study based on a generic block diagram of the receiver and consider not only narrow-band, but a wider variety of input signals. The study allows general results and conclusions that can be easily particularized to specific implementations to be obtained. Starting from the proposed model, the differential equation that describes the operation of the receiver in the linear mode is deducted and solved. Normalized parameters and functions characterizing the performance of the receiver are presented, as well as the requirements for proper operation. Several characteristic phenomena, such as hangover and multiple resonance, are described. The nonlinear behavior of the active device is also modeled to obtain a solution of the differential equation in the logarithmic mode of operation. The study is completed with a practical example operating at 2.4 GHz and illustrating the typical performance of a superregenerative receiver.**

***Index Terms*—Low power, radio receiver, RF oscillator, superregenerative receiver.**

## I. Introduction

SINCE Armstrong presented the superregenerative receiver in 1922 [1], it has been included in a variety of applications. In the 1930s, it came into widespread use by radio amateurs as an economical ultrashort-wave communications receiver. Various “walkie-talkie” communications receivers were developed based on the superregenerative principle, taking advantage of its light weight and reduced cost. With the advent of World War II, the circuit was mass-produced as a pulse responder for radar identification of ships and aircraft (I.F.F., *Identification, Friend or Foe*) [2].

As the transistor replaced the vacuum tube, the superheterodyne receiver, characterized by improved selectivity, relegated the superregenerative receiver to occasional special-purpose roles. Some examples are altitude and Doppler radar [3], [4] and solar-powered applications [5]. The superregenerative principle has also been successfully applied to optical communications [6]–[8].

Currently, the major application of the superregenerative receiver is in short-distance RF links, in which reduced cost and low power consumption are required. Among these applications are remote control systems (such as garage door openers, robotics, and model ships and airplanes), short-distance telemetry, and wireless security [9], [10]. The receiver has typically been used as a narrow-band AM receiver and, occasionally, as an FM receiver. Recently, original architectures based on the superregeneration principle have been proposed to detect spread-spectrum signals and phase- and frequency-modulated carriers [11]–[14].

In spite of the industrial interest of this receiver [15]–[17], the fundamental theory of superregenerative reception available in the literature is usually developed from particular circuits, such as the parallel *RLC* resonator coupled to a negative resistor [2], [18], [19]. An exception to this approach can be found in [10], where a general model of the receiver is proposed and simulated under a variety of operating conditions. As a novelty in this paper, the general theory of superregenerative receivers is developed analytically, starting from their generic block diagram. The study considers generic parameters, such as filter gain and damping, instead of component values. The use of this generic model is advantageous for the following reasons.

1) The receiver is split up into functional blocks, making analysis and design easier and clearer.
2) The study provides general results and conclusions.
3) The results can easily be particularized to specific designs.
4) The model may be used to compare different architectures.

From this model, the differential equation that describes the behavior of the receiver in the linear mode is obtained and solved. The characteristic parameters of the receiver are presented, as well as the conditions for proper operation. In addition, several classical concepts are reviewed or redefined in order to extend the study to the case of superregenerative receivers that operate synchronously with the received signal, such as those presented in [12] for spread-spectrum communications. The study is completed with a section dedicated to the analysis of the receiver in the logarithmic mode of operation, in which the nonlinearity of the active device is considered. Finally, we present a practical example that illustrates the typical performance of a superregenerative receiver.

Manuscript received December 30, 2003; revised April 20, 2004. This work was supported by the Spanish Dirección General de Investigación under Grant TIC2000-1015 and Grant TIC2003-02755. This paper was recommended by Associate Editor B. Maundy.

The authors are with the Department of Signal Theory and Communications, Universitat Politècnica de Catalunya, 08034 Barcelona, Spain (e-mail: moncunill@tsc.upc.edu).

Digital Object Identifier 10.1109/TCSI.2004.840095

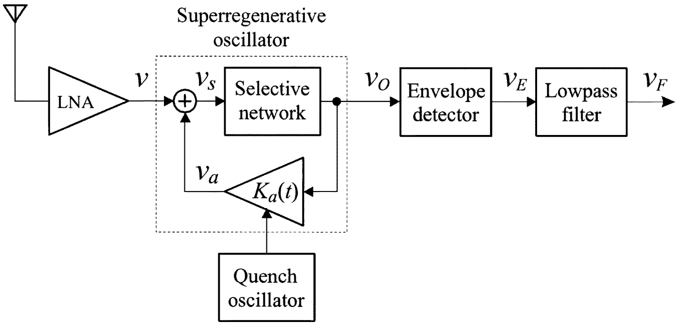


Fig. 1. Detailed block diagram of the superregenerative receiver.

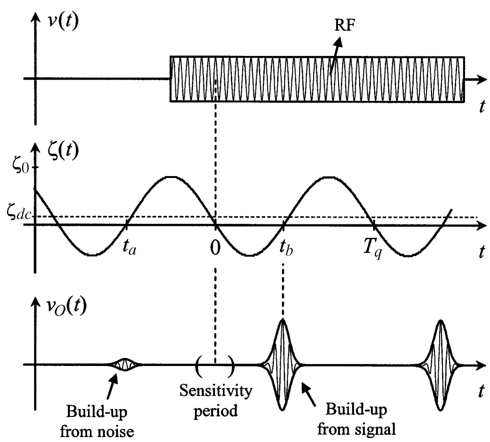


Fig. 2. RF input signal, damping function, and SRO output.

## II. Block Diagram of the Superregenerative Receiver

Oscillators are common circuits in RF communication systems, in which they usually work in a steady state, providing a constant-amplitude periodic signal. However, as dynamic circuits, oscillators exhibit transient responses before they reach their steady state of operation (for instance, when the power supply is switched on). This property is the basis of any superregenerative receiver, in which the transient response of the oscillator is used to achieve the filtering and amplification of weak signals.

The detailed block diagram of the superregenerative receiver is shown in Fig. 1, in which the input and output variables of each block represent the voltages present in the physical system. Depending on each particular case, some of these variables must be replaced by physical currents.

The core of the diagram is the *superregenerative oscillator* (SRO). It is an RF oscillator that is controlled by a low-frequency quench generator or *quench oscillator*, which causes the RF oscillations to rise and die out repeatedly. The RF oscillator can be modeled as a frequency-selective network fed back through a variable-gain amplifier. This gain is modified by the quench oscillator, making the closed-loop system alternatively unstable and stable. In this way, the signal generated in the oscillator is composed of a series of RF pulses separated by the quench period $T_q$, and the periodic build-up of the oscillations is determined by the input signal $v(t)$ (see Fig. 2).

The primary function of the *low-noise amplifier* (LNA) is to isolate the antenna from the oscillator. Otherwise, the relatively large amplitude RF pulses present in the oscillator will generate an appreciable radiated power that can cause interference in other systems. Additionally, it serves to provide better matching between the antenna and the SRO. Just as in other RF systems, the presence of this amplifier can improve overall performance in terms of noise. However, it is not indispensable for the proper operation of the receiver.

In the so-called *linear mode* of operation, the oscillations are damped before they reach their limiting equilibrium amplitude, and their peak amplitude is proportional to the amplitude of the injected signal $v(t)$. In the *logarithmic mode*, the amplitude of the oscillations is allowed to reach its limiting equilibrium value, which is determined by the nonlinearity of the feedback amplifier. In this mode of operation, the amplitude of the RF pulses remains constant, but the incremental area under the envelope is proportional to the logarithm of the amplitude of $v(t)$. In both modes of operation, the modulating input signal can be retrieved by averaging the envelope of the RF pulses. Thus, the *envelope detector* obtains the envelope of the RF signal and the *low-pass filter* removes the quench components, preserving the modulating components.

Several variants in the diagram in Fig. 1 can be proposed. For instance, the signal coming from the LNA can be added to the selective-network output instead of to the input. The envelope detector could also use the output of the feedback amplifier instead of the input. It can be shown that the performance obtained with each of those variants is quite similar. In any case, the diagram in Fig. 1 will be used hereafter, since it applies more accurately to the circuits that are commonly found in practice. Some superregenerative receivers, known as *self-quenching receivers*, generate the quench from the SRO itself. This eliminates the need for a separate quench oscillator, but offers limited control of the operation of the SRO.

### *A. Characteristic Differential Equation of the Superregenerative Receiver*

The superregenerative oscillator has been modeled as a selective network fed back through an amplifier. This amplifier has a variable gain $K_a(t)$ controlled by the quench signal, of frequency $f_q$, which causes the system to become alternatively stable and unstable. Without loss of generality, we will assume that the selective network has two dominant poles providing a bandpass response centered on $\omega_0 = 2\pi f_0$, characterized by the transfer function

$$G(s) = K_0 \frac{2\zeta_0\omega_0 s}{s^2 + 2\zeta_0\omega_0 s + \omega_0^2} \tag{1}$$

or, equivalently, by the differential equation

$$\ddot{v}_O(t) + 2\zeta_0\omega_0\dot{v}_O(t) + \omega_0^2 v_O(t) = K_0 2\zeta_0\omega_0\dot{v}_s(t) \tag{2}$$

where $\zeta_0$ is the quiescent damping factor and $K_0$ is the maximum amplification. The feedback establishes the relationship $v_s(t) = v(t) + K_a(t)v_O(t)$, which allows us to formulate the general form of the differential equation of the superregenerative receiver

$$\ddot{v}_O(t) + 2\zeta(t)\omega_0\dot{v}_O(t) + \omega_0^2 v_O(t) = K_0 2\zeta_0\omega_0\dot{v}(t) \tag{3}$$

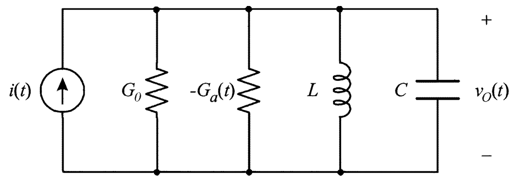


| Block diagram | $v$ | $v_O$ | $K_0$ | $\zeta_0$ | $\omega_0$ | $K_a(t)$ |
|---|---|---|---|---|---|---|
| Circuit | $i$ | $v_O$ | $\frac{1}{G_0}$ | $\frac{G_0}{2C\omega_0}$ | $\frac{1}{\sqrt{LC}}$ | $G_a(t)$ |

(a)

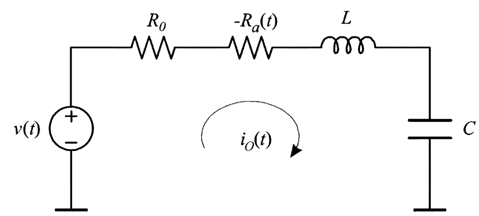


| Block diagram | $v$ | $v_O$ | $K_0$ | $\zeta_0$ | $\omega_0$ | $K_a(t)$ |
|---|---|---|---|---|---|---|
| Circuit | $v$ | $i_O$ | $\frac{1}{R_0}$ | $\frac{R_0}{2L\omega_0}$ | $\frac{1}{\sqrt{LC}}$ | $R_a(t)$ |

(b)

Fig. 3. Equivalence between the block diagram and *RLC* circuits: (a) parallel *RLC* circuit and (b) series *RLC* circuit. $G_0$ and $R_0$ include both source resistance and circuit losses.

where $\zeta(t)$ is the *instantaneous damping factor* of the closed-loop system

$$\zeta(t) = \zeta_0 \left(1 - K_0 K_a(t)\right). \tag{4}$$

Equation (3) is a linear, time-varying, second-order differential equation. If both the amplifier and the filter are noninverting (i.e., $K_a$ and $K_0$ are positive), the damping may reach the zero value. To achieve oscillation, if the amplifier is inverting, the selective network must also be inverting ($K_0$ must be negative) or a subtracter must replace the adder in the block diagram. For the sake of simplicity and unless otherwise noted, both $K_a$ and $K_0$ will be assumed positive.

By identifying the coefficients in the corresponding differential equations, it is possible to obtain the equivalence between the parameters of the block diagram (Fig. 1) and those of a particular circuit. The equivalence is shown in Fig. 3 for parallel and series *RLC* circuits. Other circuit architectures, such as the feedback oscillator studied in Section XI, can also be characterized by the model in Fig. 1.

### *B. Quench Cycle and the Damping Function*

The quench oscillator generates an instantaneous damping factor, or *damping function*, $\zeta(t)$, that is periodic (Fig. 2). This function is composed of successive *quench cycles*. A new quench cycle starts when the damping function changes to positive ($t = t_a$), which extinguishes any oscillation present in the oscillator. After it changes to negative ($t = 0$), the oscillation builds up from the injected signal $v(t)$ and achieves the maximum amplitude when $\zeta(t)$ once again changes to positive ($t = t_b$). The mathematical analysis developed below and the experimental results show that the receiver is especially sensitive to the input signal in a certain environment at the instant $t = 0$.

As we will subsequently show, the behavior of the receiver is mainly determined by the characteristics of the damping function (e.g., its shape, repetition frequency, and mean value). Since $\zeta(t)$ gives global information about the system's performance, it is a better descriptor than just the feedback gain $K_a(t)$. In practice, $K_a(t)$ is adjusted in order to obtain the desired $\zeta(t)$.

Practical damping functions have a positive dc component plus a periodic ac component, according to

$$\zeta(t) = \zeta_{dc} + \zeta_{ac}(t). \tag{5}$$

In the case of a noninverting feedback amplifier, the minimum value of $K_a(t)$ is zero and, consequently, the maximum value of $\zeta(t)$ is limited by $\zeta_0$.

## III. Solution of the Differential Equation: Linear Mode

The general solution of (3) can be broken down into the sum of the general solution of the homogeneous equation plus a particular solution of the complete equation, according to

$$v_O(t) = v_{Oh}(t) + v_{Op}(t) \tag{6}$$

where $v_{Oh}(t)$ is the free (or natural) response, which may exist even though no excitation is present, whereas $v_{Op}(t)$ represents the forced response generated by the excitation.

### *A. General Solution of the Homogeneous Equation: Free Response*

To solve the homogeneous equation

$$\ddot{v}_{Oh}(t) + 2\zeta(t)\omega_0 \dot{v}_{Oh}(t) + \omega_0^2 v_{Oh}(t) = 0 \tag{7}$$

it is convenient to make the change of variable [20]

$$\begin{aligned} v_{Oh}(t) &= u(t) e^{-\omega_0 \int_{t_a}^{t} \zeta(\lambda) d\lambda} \\ \dot{v}_{Oh} &= \left(\dot{u} - \omega_0 \zeta(t) u\right) e^{-\omega_0 \int_{t_a}^{t} \zeta(\lambda) d\lambda} \\ \ddot{v}_{Oh} &= \left(\ddot{u} - 2\omega_0 \zeta(t) \dot{u} + \left[\left(\omega_0 \zeta(t)\right)^2 - \omega_0 \dot{\zeta}(t)\right] u\right) \\ &\quad \times e^{-\omega_0 \int_{t_a}^{t} \zeta(\lambda) d\lambda} \end{aligned} \tag{8}$$

which converts the homogeneous equation into the Hill equation

$$\ddot{u}(t) + \omega_0^2 \left(1 - \zeta^2(t) - \frac{\dot{\zeta}(t)}{\omega_0}\right) u(t) = 0. \tag{9}$$

Two important restrictions must now be considered in order to simplify this equation

$$\zeta^2(t) \ll 1 \tag{10}$$

$$\left|\dot{\zeta}(t)\right| \ll \omega_0. \tag{11}$$

Restriction (10) means that the instantaneous damping factor *must be low enough* at any time and implies that the circuit is underdamped, that is, able to generate an oscillatory response. This restriction imposes that the instantaneous quality factor, defined as

$$Q(t) = \frac{1}{2\zeta(t)} \tag{12}$$

must be kept high enough in modulus. On the other hand, restriction (11) requires a *slow-variation damping function*. Both restrictions are fundamental to the proper performance of the superregenerative receiver and usually apply in practice. Thus, (9) becomes

$$\ddot{u}(t) + \omega_0^2 u(t) = 0 \tag{13}$$

which is linear, has constant coefficients, and is of known solution

$$u(t) = 2\mathrm{Re}[V_1 e^{j\omega_0 t}] = V_1 e^{j\omega_0 t} + V_1^* e^{-j\omega_0 t}. \tag{14}$$

Backing down the change of variable, we obtain the general solution of the homogeneous differential equation

$$v_{Oh}(t) = e^{-\omega_0 \int_{t_a}^{t} \zeta(\lambda) d\lambda} 2\mathrm{Re}[V_1 e^{j\omega_0 t}]. \tag{15}$$

### B. Particular Solution of the Complete Equation: Forced Response

The particular solution can be found by the method of variation of parameters [21]

$$v_{Op}(t) = 2\mathrm{Re}\left[V_2(t) b(t)\right] = V_2(t)b(t) + V_2^*(t) b^*(t) \tag{16}$$

where $b(t)$ is the base of the homogeneous equation

$$b(t) = e^{-\omega_0 \int_{t_a}^{t} \zeta(\lambda) d\lambda} e^{j\omega_0 t}. \tag{17}$$

As the method of variation of parameters states, the particular solution fulfills the complete equation if

$$\begin{aligned} \dot{V}_2 b + \dot{V}_2^* b^* &= 0 \\ \dot{V}_2 \dot{b} + \dot{V}_2^* \dot{b}^* &= 2K_0 \zeta_0 \omega_0 \dot{v}. \end{aligned} \tag{18}$$

This system of equations provides the derivative of the intended function

$$\dot{V}_2(t) = -jK_0\zeta_0 \frac{\dot{v}(t)}{b(t)} \tag{19}$$

which, after integration, results in

$$\begin{aligned} V_2(t) &= -jK_0\zeta_0 \int_{t_a}^{t} \frac{\dot{v}(\tau)}{b(\tau)} d\tau \\ &= -jK_0\zeta_0 \int_{t_a}^{t} \dot{v}(\tau) e^{\omega_0 \int_{t_a}^{\tau} \zeta(\lambda) d\lambda} e^{-j\omega_0 \tau} d\tau. \end{aligned} \tag{20}$$

Now, taking two times the real part of $V_2(t)b(t)$, according to (16), leads to the expression of the particular solution

$$\begin{aligned} v_{Op}(t) &= e^{-\omega_0 \int_{t_a}^{t} \zeta(\lambda) d\lambda} \\ &\times 2\mathrm{Re}\left[-jK_0\zeta_0 \int_{t_a}^{t} \dot{v}(\tau) e^{\omega_0 \int_{t_a}^{\tau} \zeta(\lambda) d\lambda} e^{-j\omega_0(\tau - t)} d\tau\right]. \end{aligned} \tag{21}$$

### C. Compact Expression of the Solution

In order to obtain compact expressions that are easier to interpret, let us introduce several parameters and functions that have been used in the literature to describe the operation of the receiver [2], [18] and whose meaning will subsequently be explained:

1) *Superregenerative gain*:

$$K_s = e^{-\omega_0 \int_0^{t_b} \zeta(\lambda) d\lambda}. \tag{22}$$

2) *Normalized envelope of the SRO output*:

$$p(t) = e^{-\omega_0 \int_{t_b}^{t} \zeta(\lambda) d\lambda}. \tag{23}$$

3) *Sensitivity curve*:

$$s(t) = e^{\omega_0 \int_0^{t} \zeta(\lambda) d\lambda}. \tag{24}$$

All of these functions exhibit an exponential dependence on the damping function $\zeta(t)$. With the notation introduced above, it is possible now to express the general solution of the homogeneous differential equation of the superregenerative receiver as

$$v_{Oh}(t) = V_h p(t) \cos(\omega_0 t + \phi_h) \tag{25}$$

where $V_h$ and $\phi_h$ are related to the modulus and the angle, respectively, of the previously introduced complex constant $V_1$. The particular solution of the complete equation becomes

$$v_{Op}(t) = 2\zeta_0 K_0 K_s p(t) \int_{t_a}^{t} \dot{v}(\tau) s(\tau) \sin \omega_0 (t - \tau) d\tau. \tag{26}$$

The above expressions apply to any value of $t$. In Section IV, however, we will be interested in the values of $s(t)$ in the interval $(t_a, t_b)$. Note that the maximum value of expression (24) within this interval equals unity and that this value is achieved when $t = 0$. Regarding $p(t)$, we will be interested in the corresponding values when $t > 0$. In this case, (23) shows that the maximum value of unity is achieved when $t = t_b$. Fig. 4 shows the typical shapes of $s(t)$ and $p(t)$ under sinusoidal quench.

## IV. Response to an RF Pulse

Next, we will investigate the system response to a single RF pulse. The results of this analysis are of great importance, for they can be extended to a variety of practical excitations. For

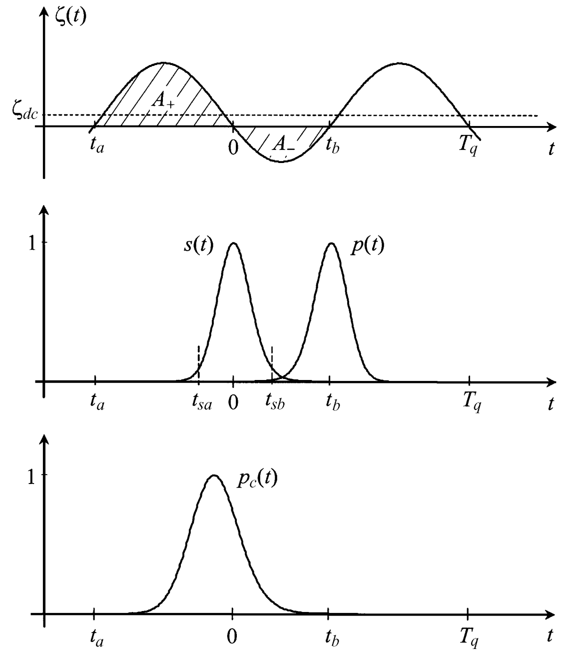


Fig. 4. SRO damping function $\zeta(t)$, sensitivity curve $s(t)$, normalized envelope of the output pulse $p(t)$, and normalized envelope of the input signal $p_c(t)$. Outside of the interval defined by $t_{sa}$ and $t_{sb}$, the sensitivity of the receiver to the input signal becomes negligible.

the sake of simplicity, noise will be neglected in this study. Additional information about the influence of noise according to the model presented in this paper is available in [13].

Let us assume that an RF pulse is applied within the limits of a single quench cycle, given by the interval $(t_a, t_b)$, and expressed as

$$v(t) = Vp_c(t)\cos(\omega t + \phi) \tag{27}$$

where $p_c(t)$ is the normalized pulse envelope (Fig. 4) and $V$ its peak amplitude. $p_c(t)$ is assumed to be zero beyond the cycle limits defined by $t_a$ and $t_b$. Although in many practical cases $p_c(t)$ may be assumed to be constant and to represent a fraction of the input signal (this is the case of conventional receivers operating with narrow-band modulation), in others it may be a relatively slow-variation function (for instance, a return-to-zero chip pulse in a spread-spectrum receiver [22]). Our formulation allows for this possibility. We consider in our reasoning that there is no free response coming from previous quench cycles when the current cycle starts, that is, $v_{Oh}(t) = 0$ and, therefore, $v_O(t) = v_{Op}(t)$. We can see from (26) that the response $v_{Op}(t)$ is determined by the derivative of the excitation, whose expression is

$$\dot{v}(t) = V\left[\dot{p}_c(t)\cos(\omega t + \phi) - p_c(t)\omega\sin(\omega t + \phi)\right]. \tag{28}$$

This expression can be approximated by

$$\dot{v}(t) \approx -Vp_c(t)\omega\sin(\omega t + \phi) \tag{29}$$

when $p_c(t)$ varies slowly in comparison with the RF oscillation ($|\dot{p}(t)| \ll p(t)\omega$). Taking $v_{Oh}(t) = 0$ and replacing (29) in (26), (6) yields

$$\begin{aligned} v_O(t) \approx &-2VK_0K_s\zeta_0\omega p(t) \\ &\times \int_{t_a}^{t} p_c(\tau)s(\tau)\sin(\omega\tau + \phi)\sin\omega_0(t-\tau)d\tau \\ &= VK_0K_s\zeta_0\omega p(t)\int_{t_a}^{t} p_c(\tau)s(\tau) \\ &\times \left[\cos\left((\omega-\omega_0)\tau + \omega_0 t + \phi\right)\right. \\ &\left. -\cos\left((\omega+\omega_0)\tau - \omega_0 t + \phi\right)\right]d\tau. \end{aligned} \tag{30}$$

Since $p_c(t)$ and $s(t)$ are slow-variation functions compared to the RF oscillation, the integral will exhibit a significant value when one of the cosine addends becomes a low-frequency term, that is, when $\omega \approx \omega_0$ or $\omega \approx -\omega_0$. If we take $\omega \geq 0$, then the cosine whose frequency is $\omega + \omega_0$ will generate a negligible component. Hence, we can write

$$\begin{aligned} v_O(t) \approx &\, VK_0K_s\zeta_0\omega p(t) \\ &\times \int_{t_a}^{t} p_c(\tau)s(\tau)\cos\left((\omega-\omega_0)\tau + \omega_0 t + \phi\right)d\tau. \end{aligned} \tag{31}$$

This leads us to consider that the sensitivity curve usually decreases rapidly as time separates from the origin, $t = 0$, reaching negligible values that fall outside of the interval defined by $(t_{sa}, t_{sb})$ in Fig. 4, which can be defined as the *sensitivity period*. This means that the influence of the input signal is very small outside the specified interval. Assuming that $s(t)$ is small at the end of the quench period, it has an effect on both the initial value of the envelope and the superregenerative gain. In particular, we can show that

$$s(t_b) = p(0) = e^{\omega_0\int_0^{t_b}\zeta(\lambda)d\lambda} = \frac{1}{K_s} \ll 1. \tag{32}$$

Therefore, a small value for the sensitivity curve at the end of the quench cycle implies small values for the output envelope near the origin and large superregenerative gains. If we consider that the sensitive period ends for all practical purposes when the amplitude of the oscillation is still small, we can replace $t$ by $t_b$ in the integration limits of (31), yielding

$$\begin{aligned} v_O(t) = VK_0K_s\zeta_0\omega p(t)\int_{t_a}^{t_b} p_c(\tau)s(\tau)\cos\left((\omega-\omega_0)\tau\right. \\ \left. +\omega_0 t + \phi\right)d\tau. \end{aligned} \tag{33}$$

Note that this equation is valid only after the practical end of the sensitivity period, when $t > t_{sb}$; otherwise, $t$ must be kept instead of $t_b$. Since $p_c(t)$ is zero out of the integration limits, the latter can be extended from $-\infty$ to $+\infty$. In this way, as shown in the subsequent sections, $v_O(t)$ is (approximately) proportional to the real part of the Fourier transform of the pulse envelope $p_c(t)$ weighted by the sensitivity curve $s(t)$. Expression (33) shows that, in the linear mode, the output of the oscillator is proportional to the peak amplitude of the input signal, and that the forced response has the form of the free response after the end of the sensitivity period [cf. (44)].

### *A. Response to a Pulse When the Carrier is Tuned to the Resonance Frequency*

When the receiver is tuned to the received frequency, then the solution

$$v_O(t) = VK_0K_s\zeta_0\omega_0 p(t)\left[\int_{t_a}^{t_b} p_c(\tau)s(\tau)d\tau\right]\cos(\omega_0 t+\phi) \tag{34}$$

demonstrates that, in addition to $K_0$ and $K_s$, a new amplification factor appears. This factor is the *regenerative gain*

$$K_r = \zeta_0\omega_0\int_{t_a}^{t_b} p_c(\tau)s(\tau)d\tau. \tag{35}$$

This gain takes into account the area of the envelope of the received pulse weighted by the sensitivity curve. A pulse that concentrates its energy around the peak of the sensitivity curve will have a regenerative gain greater than that of a more spread pulse. Thus, the new expression for the tuned input is

$$v_O(t) = VK_0K_rK_s p(t)\cos(\omega_0 t+\phi). \tag{36}$$

This expression allows the peak amplification $K$, defined as the ratio between the peak values of the input and output oscillations, to be obtained. Thus

$$K = K_0K_rK_s. \tag{37}$$

The output is then reduced to the simple expression

$$v_O(t) = VKp(t)\cos(\omega_0 t+\phi). \tag{38}$$

### *B. Response to a Pulse With Arbitrary Carrier Frequency*

By taking into account the regenerative gain, the general response of the receiver to an excitation of arbitrary frequency (33) can be rewritten as

$$\begin{aligned} v_O(t) =& VKp(t)\frac{\omega}{\omega_0} \\ &\times\frac{\int_{t_a}^{t_b} p_c(\tau)s(\tau)\cos\left((\omega-\omega_0)\tau+\omega_0 t+\phi\right)d\tau}{\int_{t_a}^{t_b} p_c(\tau)s(\tau)d\tau} \\ =& VKp(t)\frac{\omega}{\omega_0} \\ &\times\frac{\mathrm{Re}\left[\left(\int_{t_a}^{t_b} p_c(\tau)s(\tau)e^{j(\omega-\omega_0)\tau}d\tau\right)e^{j(\omega_0 t+\phi)}\right]}{\int_{t_a}^{t_b} p_c(\tau)s(\tau)d\tau}. \end{aligned} \tag{39}$$

Defining the complex function

$$\psi(\omega) = \int_{-\infty}^{\infty} p_c(t)s(t)e^{j\omega t}dt \tag{40}$$

or, equivalently

$$\psi(\omega) = \left[\int_{-\infty}^{\infty} p_c(t)s(t)e^{-j\omega t}dt\right]^* = F^*\left\{p_c(t)s(t)\right\} \tag{41}$$

where the operator $F$ denotes the Fourier transform, and taking into account that $p_c(t)$ is null out of the interval $(t_a, t_b)$, the response can be rewritten as

$$\begin{aligned} v_O(t) =& VKp(t)\frac{\omega}{\omega_0}\frac{\mathrm{Re}\left[\psi(\omega-\omega_0)e^{j(\omega_0 t+\phi)}\right]}{\psi(0)} \\ =& VKp(t)\frac{\omega}{\omega_0}\frac{|\psi(\omega-\omega_0)|}{\psi(0)} \\ &\times\cos\left(\omega_0 t+\phi+\angle\psi(\omega-\omega_0)\right). \end{aligned} \tag{42}$$

Note that $\psi(0)$ is real since both $p_c(t)$ and $s(t)$ are real functions. By defining the frequency-dependent function

$$H(\omega) = \frac{\omega}{\omega_0}\frac{\psi(\omega-\omega_0)}{\psi(0)} \tag{43}$$

we obtain the general expression of the oscillator output of the superregenerative receiver

$$v_O(t) = VK\left|H(\omega)\right|p(t)\cos\left(\omega_0 t+\phi+\angle H(\omega)\right). \tag{44}$$

Therefore, $H(\omega)$, which is a bandpass function centered on the resonance frequency $\omega_0$, determines the frequency response of the receiver. The function $\psi(\omega)$ can be understood as a low-pass equivalent of the bandpass response. With reference to (44), we must emphasize the following:

1) the response is proportional to the amplitude of the input signal, $V$;
2) this response is generated only by the signal present in $t_a < t < t_b$;
3) the expression holds only after the sensitivity period ($t > t_{sb}$).

## V. Characteristic Parameters of the Receiver

Table I gathers the expressions of the characteristic parameters and functions of the superregenerative receiver, as well as the restrictions on their validity. Let us explain their meaning in depth.

### *A. Feedforward Gain*

Factor $K_0$ is the gain provided by the selective network at the resonance frequency. It represents the open-loop gain of the superregenerative oscillator, i.e., the one provided when the feedback amplifier remains inactive.

### *B. Sensitivity Curve*

The sensitivity curve $s(t)$ is a normalized function that decreases toward zero as time separates from $t = 0$, the instant

TABLE I
SUMMARY OF THE PARAMETERS AND FUNCTIONS THAT CHARACTERIZE THE SUPERREGENERATIVE RECEIVER

| | | |
|---|---|---|
| **BLOCK PARAMETERS** | | |
| Selective network $G(s)=K_0\dfrac{2\zeta_0\omega_0 s}{s^2+2\zeta_0\omega_0 s+\omega_0^2}$; Periodic feedback gain $K_a(t)$ | $\Rightarrow$ | Periodic closed-loop damping factor $\zeta(t)=\zeta_0(1-K_0K_a(t))$ |
| **INPUT SIGNAL** | | |
| $v(t)=V\,p_c(t)\cos(\omega t+\phi)\,,\quad t_a<t<t_b$ | | |
| Restrictions: $\zeta^2(t)<<1\,,\ \lvert\dot{\zeta}(t)\rvert<<\omega_0\,,\ \lvert\dot{p}_c(t)\rvert<<p_c(t)\,\omega\,,\ \omega\geq 0$ | | |
| **RESPONSE** | | |
| $v_O(t)=VK\lvert H(\omega)\rvert\,p(t)\cos(\omega_0 t+\phi+\angle H(\omega))\,,\quad t>t_{sb}\,,$ | | |
| with the following parameters: | | |
| Peak gain | $\rightarrow$ | $K=K_0K_rK_s$ |
| Regenerative gain | $\rightarrow$ | $K_r=\zeta_0\omega_0\int_{t_a}^{t_b}p_c(\tau)\,s(\tau)\,d\tau\,,\quad s(t)=e^{\omega_0\int_0^t\zeta(\lambda)d\lambda}$ |
| Superregenerative gain | $\rightarrow$ | $K_s=e^{-\omega_0\int_0^{t_b}\zeta(\lambda)d\lambda}$ |
| Frequency response | $\rightarrow$ | $H(\omega)=\dfrac{\omega}{\omega_0}\dfrac{\psi(\omega-\omega_0)}{\psi(0)}\,,\quad \psi(\omega)=F^*\{p_c(t)s(t)\}$ |
| Normalized oscillation envelope | $\rightarrow$ | $p(t)=e^{-\omega_0\int_{t_b}^{t}\zeta(\lambda)d\lambda}$ |

in which it takes the maximum value of unity. This curve is directly related to the *time aperture function* defined in [23] and [19]. The decrease of the sensitivity curve is quite fast, due to its exponential dependence on $t$. In practical receivers, the value of this function becomes practically null in an environment relatively close to the origin, $t=0$. The shape of $s(t)$ is determined mainly by the environment of the zero-crossing of $\zeta(t)$. A slow transition will provide a wide sensitivity curve, whereas a fast one will generate a narrow curve.

Both the regenerative gain and the frequency response depend on the product $p_c(t)s(t)$. In this way, the sensitivity curve acts as a function that weights the incoming envelope $p_c(t)$; the values of $p_c(t)$ near $t=0$ will be taken into account, whereas those close to $t_a$ and $t_b$ will be irrelevant. The instant $t=0$ can be considered the instant of maximum sensitivity.

### C. Regenerative Gain

$K_r$ is the regenerative gain, also called the *slope* or *step factor* in the literature, depending on the type of quench applied [2]. It takes into account the contribution of differential portions of the input signal envelope, each one weighted by the sensitivity curve. This gain depends on the product $p_c(t)s(t)$. If $p_c(t)$ or $s(t)$ is narrow, the regenerative gain will be small. If both $p_c(t)$ and $s(t)$ are wide, the regenerative gain will be large.

### D. Superregenerative Gain

The superregenerative gain $K_s$ is associated with the exponential growth of the oscillation and is the most significant amplification factor. It is determined by the area enclosed by the negative portion of the damping function.

### E. Frequency Response

The frequency response is the normalized Fourier transform of $p_c(t)s(t)$ shifted toward the oscillation frequency $\omega_0$. If both $p_c(t)$ and $s(t)$ are wide, the bandwidth of the selectivity curve of the receiver will be small; if $p_c(t)$ or $s(t)$ is narrow, the bandwidth will be large.

### F. Normalized Oscillation Envelope

Finally, the normalized oscillation envelope $p(t)$ is determined mainly by the evolution of the damping function close to $t=t_b$. The same conclusions obtained for the sensitivity curve apply in this case, in the environment of $t_b$.

## VI. RESPONSE IN THE SINUSOIDAL STEADY STATE

Consider next the receiver excited with a single tone

$$v(t)=V\cos(\omega t+\phi). \tag{45}$$

In order to take advantage of results obtained in the previous section, we express $v(t)$ as a superposition of RF pulses, according to

$$v(t)=V\sum_{m=-\infty}^{\infty}p_c(t-mT_q)\cos\left(\omega(t-mT_q)+m\omega T_q+\phi\right) \tag{46}$$

where $p_c(t-mT_q)$ is a rectangular pulse of unitary amplitude allocated in the $m$th quench period. The response to this excitation can be obtained by the superposition of single responses, yielding

$$v_O(t)=VK\left|H(\omega)\right|\sum_{m=-\infty}^{\infty}p(t-mT_q)\times\cos\left(\omega_0 t+m(\omega-\omega_0)T_q+\phi+\angle H(\omega)\right). \tag{47}$$

This expression shows that the oscillator output is composed of a series of RF pulses. In addition, we can see that, if the received frequency differs from the natural frequency of the oscillator ($\omega\neq\omega_0$), the output phase varies from one pulse to the next. When $\omega=\omega_0$, all of the pulses are in phase.

## VII. RESPONSE TO A GENERIC BANDPASS MODULATION

Let us now consider the circuit response to the generic bandpass excitation

$$v(t)=\sum_{m=-\infty}^{\infty}V_m p_c(t-mT_c)\cos(\omega_m t+\phi_m). \tag{48}$$

This expression may represent a wide class of narrow-band and wide-band modulations, including amplitude, frequency, and phase-shift keying. Let us assume that the quench period equals the received-pulse period $T_q = T_c$ and that perfect synchronism exists, so that the pulse $p_c(t - mT_q)$ matches the $m$th quench period. In the case of conventional receivers operating under narrow-band modulation, this assumption is merely a mathematical artifice. In certain novel applications of the receiver, synchronism is kept by means of a synchronization loop that controls the frequency of the quench oscillator [13], [14]. Expressing (48) as

$$v(t) = \sum_{m=-\infty}^{\infty} V_m p_c(t - mT_q) \cos(\omega_m (t - mT_q) + m\omega_m T_q + \phi_m) \tag{49}$$

allows the complete response to be obtained by superposition, yielding

$$\begin{aligned} v_O(t) = &K \sum_{m=-\infty}^{\infty} V_m \left| H(\omega_m) \right| p(t - mT_q) \\ &\times \cos(\omega_0 t + m(\omega_m - \omega_0)T_q + \phi_m + \angle H(\omega_m)). \end{aligned} \tag{50}$$

This expression shows that the oscillator output is composed of a series of RF pulses of frequency $\omega_0$. In particular, for ASK modulation, we have $\omega_m = \omega$, $\phi_m = \phi$, and so the amplitude variations at the input appear at the output. Hence, ASK signals will provide ASK responses. For PSK modulation, we have $V_m = V$ and $\omega_m = \omega$. Here, the term $m(\omega - \omega_0)T_q + \angle H(\omega)$ is introduced in the output phase. This term is null when $\omega = \omega_0$, a situation in which the receiver tracks the input phase. For FSK modulation, $V_m = V$ and $\phi_m$ can be variable, in order to provide a continuous or fixed phase. In this case, the output exhibits amplitude and phase modulation through $H(\omega)$, but the frequency is always $\omega_0$. This behavior explains the characteristic FM-to-AM conversion in superregenerative receivers.

## VIII. Hangover and Multiple Resonance

Under normal receiver operation, the output oscillation in a given quench cycle is generated mainly from the incoming signal and not from the remnant of the previous cycle. This implies that sufficient damping must be applied at the beginning of the cycle to extinguish that remnant. In this case, the oscillation in the current cycle depends only on the signal injected within the corresponding sensitivity period. This applies also in the absence of a signal, when the RF oscillation builds up from noise, showing a random amplitude and phase. When this behavior takes place, the receiver is said to be in a *noncoherent state of operation*. However, if the output pulse lasts more than one quench period, it will overlap other pulses. In this case, the output in a given cycle depends significantly on that of the preceding cycles, and the receiver is said to operate with appreciable *hangover*. In general, this effect is undesirable, because it produces a sort of intersymbol interference. When hangover is strong, the signal growth is determined by the preceding remnant rather than by the incoming signal. In this case, the output phase is the same from one cycle to another, and the receiver is said to operate in a *coherent state of oscillation* [2]. In this situation, it shows little or no sensitivity to the excitation.

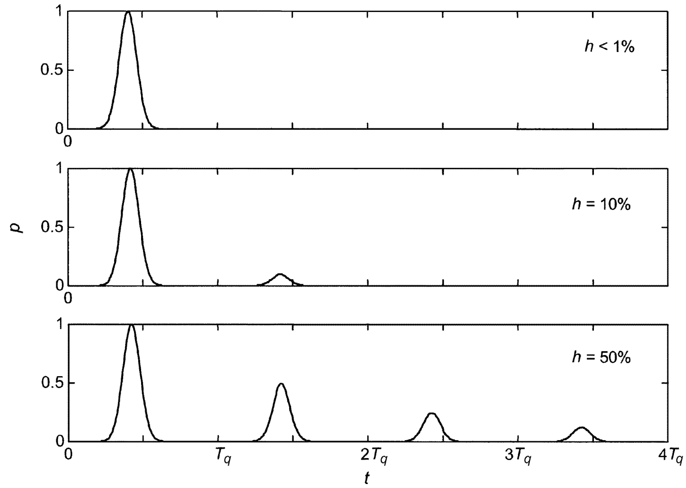


Fig. 5. Effect of hangover in the envelope of the SRO output for different values of $h$.

To quantitatively evaluate the influence of hangover, let us split up the damping function into the dc and ac components according to (5), so that we can write

$$p(t) = e^{-\omega_0 \int_{t_b}^{t} \zeta(\lambda) d\lambda} = e^{-\omega_0 \zeta_{dc}(t - t_b)} e^{-\omega_0 \int_{t_b}^{t} \zeta_{\mathrm{ac}}(\lambda) d\lambda}. \tag{51}$$

Note that the first exponential in the product decreases with a time constant equal to $1/(\omega_0 \zeta_{\mathrm{dc}})$, whereas the second exponential is a periodic function. It is possible to define the *hangover coefficient* as the ratio between the amplitudes of the second (undesired) peak and that of the first one

$$h = \frac{p(t_b + T_q)}{p(t_b)} = e^{-\omega_0 \zeta_{\mathrm{dc}} T_q} = e^{-2\pi \zeta_{\mathrm{dc}} \frac{f_0}{f_q}}. \tag{52}$$

The hangover coefficient depends not on the shape but on the mean value of the damping function. Note that $\zeta_{\mathrm{dc}} T_q$ is the area enclosed by the mean value of $\zeta(t)$ in one quench period or, equivalently, the difference between the areas $A_+$ and $A_-$ in Fig. 4. This difference must be kept large enough in order to reduce hangover. Fig. 5 shows the pulse envelope for several hangover coefficients. For $h < 0.01$, only one significant peak appears. For $h = 0.1$, a second maximum is observed, and, for $h = 0.5$, the pulse lasts many quench periods.

The overlapping effect of successive pulses due to hangover also becomes evident in the sinusoidal steady state. In this case, the additional factor

$$F(\omega) = \frac{1}{1 - h e^{-j(\omega - \omega_0)T_q}} \tag{53}$$

must be included in the frequency response (see the Appendix). This factor generates multiple peaks in the frequency response, as shown in Fig. 6, an effect known as *multiple resonance* [24].

### A. Conditions for Negligible Hangover

Note that the hangover coefficient is reduced by increases in the mean value of the damping function $\zeta_{\mathrm{dc}}$ and/or the ratio $f_0/f_q$. This implies that, at low quench frequencies, $\zeta_{\mathrm{dc}}$ can be small. At high quench frequencies, $\zeta_{\mathrm{dc}}$ must be increased in order to compensate for the decrease in $f_0/f_q$. In any case, if

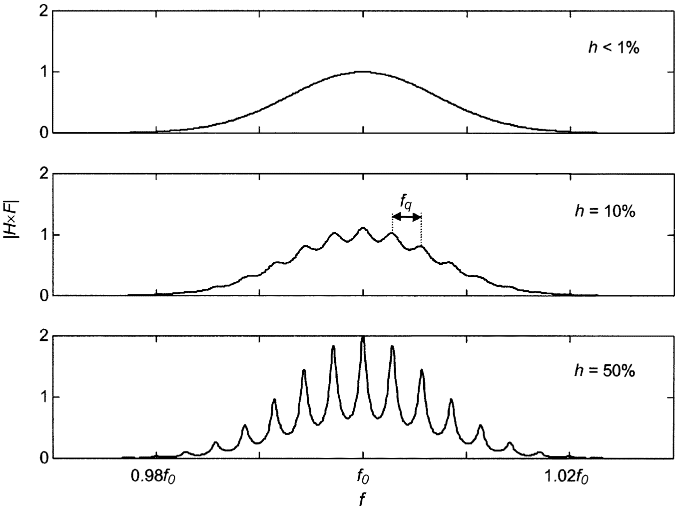


Fig. 6. Effect of hangover in the frequency response for different values of $h$ (sinusoidal steady state).

the goal is to keep the hangover coefficient below a given value $h$, the condition

$$\zeta_{\rm dc} > \frac{f_q}{2\pi f_0} \ln \frac{1}{h} \tag{54}$$

must be satisfied, a condition that is more restrictive at high quench frequencies.

## IX. Envelope Detection and Low-Pass Filtering

Superregenerative receivers are intended to be simple receivers. Hence, they usually work as noncoherent receivers, and the information is retrieved from the envelope of the RF oscillation. In this case, the phase information is lost, which implies that the receiver is suitable for ASK and FSK. The output voltage of the envelope detector is obtained mathematically by simply removing the cosine term in (44). We will assume that a linear-law detector with a detection constant $K_E = 1$ is used. Thus, we obtain for a single quench interval

$$v_E(t) = VK\,|H(\omega)|\,p(t) \tag{55}$$

and

$$v_E(t) = K \sum_{m=-\infty}^{\infty} V_m\,|H(\omega_m)|\,p(t - mT_q) \tag{56}$$

for the bandpass excitation defined by (48). Next, the low-pass filter (an integrator in spread-spectrum architectures) removes the components associated with the quench frequency $f_q$ and extracts the average (or the integral) of $v_E(t)$. If the filter has a bandwidth equal to $f_{lpf}$, it may be assumed that approximately $N = f_q/f_{lpf}$ pulses are averaged (or integrated). Thus, the filtered envelope provides an output whose instantaneous value depends on the $N$ previous pulses.

In the case of the sinusoidal steady state, a simple expression for $v_F(t)$ can be found. Taking $V_m = V$, $\omega_m = \omega$, and assuming, for simplicity's sake, a filter amplification $K_F = 1$, we have

$$v_F(t) = VK\,|H(\omega)|\,\overline{p(t)} = VK_{\rm eff}\,|H(\omega)| \tag{57}$$

where the factor $K_{eff}$ is the *effective amplification* introduced by the receiver, including the envelope detection and low-pass filtering operations

$$K_{\rm eff} = K\overline{p(t)} = K_0 K_r K_s \overline{p(t)}. \tag{58}$$

Equation (57) is extensible to amplitude modulations ($V = V(t)$) whose modulation bandwidth is within the low-pass filter bandwidth. This is the case of narrow-band superregenerative receivers.

## X. Operation in the Logarithmic Mode

The logarithmic mode of operation appears when the amplitude of the oscillation is large enough (typically from hundredths of a volt to one volt in transistor oscillators) for the nonlinearity of the feedback amplifier to become relevant. This nonlinearity limits the build-up of the oscillation and modifies the behavior of the receiver. Generally, the analysis of the transient build-up of oscillations in an oscillator to their equilibrium amplitude is quite complex. In the case of superregenerative receivers, yet another difficulty is the fact that damping varies during the build-up. Consequently, different simplifications have been made in the literature to describe the evolution of the oscillation. In some cases, the oscillator is considered linear until the amplitude of the oscillation is limited at the equilibrium value [2], [10], [18]. In others, nonlinear differential equations are solved considering the simplest case of constant damping during the build-up [25]. As a novelty in this section, a more accurate and realistic solution that is valid for any quench waveshape is obtained analytically for the nonlinear differential equation.

### A. Average Large-Signal Amplification of the Feedback Amplifier

First of all, let us consider the performance of a nonlinear amplifier providing fixed small-signal gain. The amplifier's nonlinearity can be expressed in a general form as

$$v_a = f(v_O). \tag{59}$$

We assume that both $v_a$ and $v_O$ are incremental variables that, in practical circuits, must be superimposed on bias or quiescent values. According to this assumption, the nonlinear function must accomplish $f(0) = 0$. For a small value of $v_O$, we have $v_a \approx K_a v_O$, thus $K_a$ represents the small-signal amplification. Nevertheless, when a sinusoidal excitation with relatively large amplitude $v_E$ is applied to the input of the amplifier

$$v_O(t) = v_E \cos(\omega_0 t + \phi_0) \tag{60}$$

the response exhibits rich harmonic content, according to the Fourier series expansion

$$v_a(t) = c_0(v_E) + \sum_{n=1}^{\infty} 2\,|c_n(v_E)| \cos\left(n\omega_0 t + \arg c_n(v_E)\right) \tag{61}$$

where $c_n$'s are the complex coefficients of the exponential form of the series. Obviously, these coefficients depend on the input amplitude $v_E$. Although the output of the amplifier may be rich in harmonics, only the fundamental component contributes significantly to generating a response at the output of the selective network. The other components are filtered out, provided that the quality factor of the selective network is large ($Q_0 \gg 1$). As a result, only the fundamental component of the amplifier output must be considered in order to determine the behavior of the closed-loop system. It can be easily demonstrated that the fundamental component of $v_a$ is in phase with the input $v_O$. Indeed, by making an appropriate change of variable, we have

$$c_1(v_E) = \frac{1}{T}\int_{t_1}^{t_1+T} f\left(v_E \cos(\omega_0 t + \phi_0)\right) e^{-j\omega_0 t} dt = e^{j\phi_0}\frac{1}{T}\int_{\tau_1}^{\tau_1+T} f(v_E \cos\omega_0\tau) e^{-j\omega_0\tau} d\tau \quad (62)$$

where the second integral must be real, since the nonlinear function $f(v_E \cos\omega_0\tau)$ is even. Hence, we can state that the output phase equals the input phase

$$\arg c_1(v_E) = \phi_0. \quad (63)$$

Instead of the small-signal amplification used in previous sections, it is convenient to define the *average large-signal amplification* $K_{\text{al}}$, which is equal to the ratio of the fundamental component of the amplifier output to the fundamental driving input

$$K_{\text{al}}(v_E) = \frac{2\left|c_1(v_E)\right|}{v_E}. \quad (64)$$

With this new parameter, the behavior of the amplifier turns out to be similar to that of the small-signal amplifier. The basic difference is that $K_{\text{al}}$ is a function of $v_E$ and no longer a constant.

Let us now consider the effect produced by the quench operation. Under small-signal operation, the quench signal modifies the characteristics of the amplifier in order to generate a periodic amplification $K_a(t)$. When the signal becomes large, the nonlinear function defined by (59) changes over time and must be replaced by

$$v_a = f(t, v_O). \quad (65)$$

In the same way, the Fourier coefficients in (61) will depend on the instantaneous quench and therefore on time. In this case, the series expansion makes sense, provided that the quench varies slowly enough in comparison to the high-frequency oscillation, as usually occurs. Finally, the average large-signal amplification also depends on time, as follows:

$$K_{\text{al}}(t, v_E) = \frac{2\left|c_1(t, v_E)\right|}{v_E}. \quad (66)$$

### B. Differential Equation of the Oscillation Envelope After the Sensitivity Period

By applying a harmonic balance criterion, we have concluded that only the effective large-signal amplification must be taken into account to obtain the selective-network output. In this way, the closed-loop differential equation of the system becomes

$$\ddot{v}_O(t) + 2\zeta_l(t, v_E)\omega_0\dot{v}_O(t) + \omega_0^2 v_O(t) = K_0 2\zeta_0\omega_0\dot{v}(t) \quad (67)$$

where $\zeta_l(t, v_E)$ is the *average large-signal damping function*, which depends on the amplitude of the oscillation $v_E$ according to

$$\zeta_l(t, v_E) = \zeta_0\left(1 - K_0 K_{\text{al}}(t, v_E)\right). \quad (68)$$

We must note that the nonlinear effects usually take place after the sensitivity period, when the oscillator response becomes large and is expressed as

$$v_O(t) = v_E(t)\cos(\omega_0 t + \phi_0). \quad (69)$$

Therefore, since the influence of the excitation becomes negligible after $t = t_{sb}$, (67) is reduced to the homogeneous equation

$$\ddot{v}_O(t) + 2\zeta_l(t, v_E)\omega_0\dot{v}_O(t) + \omega_0^2 v_O(t) = 0. \quad (70)$$

Assuming that the envelope $v_E(t)$ is a slow-variation function, we have

$$\begin{aligned}\dot{v}_O &= \dot{v}_E\cos(\omega_0 t + \phi_0) - v_E\omega_0\sin(\omega_0 t + \phi_0)\\ \ddot{v}_O &= -2\dot{v}_E\omega_0\sin(\omega_0 t + \phi_0) - v_E\omega_0^2\cos(\omega_0 t + \phi_0)\end{aligned} \quad (71)$$

where the second derivative $\ddot{v}_E$ has been neglected, since it is of a smaller order of magnitude. By substituting (71) in (70), we obtain

$$\left[\zeta_l(t, v_E)\cos(\omega_0 t + \phi_0) - \sin(\omega_0 t + \phi_0)\right]\dot{v}_E - \zeta_l(t, v_E)\omega_0\sin(\omega_0 t + \phi_0)v_E = 0. \quad (72)$$

As the large-signal amplification $K_{\text{al}}(t, v_E)$ is normally a "compressed" version of $K_a(t)$ [see (78)], so the average damping $\zeta_l(t, v_E)$ is compressed with regard to $\zeta(t)$. Hence, the average damping accomplishes $|\zeta_l(t, v_E)| \ll 1$ and the cosine in (72) can be neglected, yielding

$$\dot{v}_E(t) + \zeta_l(t, v_E)\omega_0 v_E(t) = 0. \quad (73)$$

Equation (73) is the differential equation that governs the oscillation envelope after the sensitivity period. To verify the consistency of this expression, let us show that, by replacing $\zeta_l(t, v_E)$ with $\zeta(t)$, the equation becomes

$$\dot{v}_E + \zeta(t)\omega_0 v_E = 0 \quad (74)$$

whose solution takes the form previously obtained for the linear mode

$$v_E(t) = V_h e^{-\omega_0\int_{t_b}^{t}\zeta(\lambda)d\lambda} = VKp(t). \quad (75)$$

### C. Approximate Solution of the Differential Equation

In order to solve (73), we must know the function $\zeta_l(t, v_E)$. Although in many practical cases the solution must be obtained by numerically solving the differential equation, we subsequently provide an analytical solution that represents the behavior of the receiver in this mode of operation quite accurately. In this way, let us approximate the nonlinearity of the amplifier by the third-order polynomial

$$v_a = f(v_O) \approx K_a v_O + a_2 v_O^2 + a_3 v_O^3 \tag{76}$$

where the independent term $a_0$ is assumed to be included in the incremental variable $v_a$. The third-order term must be considered, since the second-order term does not generate any fundamental-frequency component. Taking $v_O = v_E \cos(\omega_0 t + \phi)$, we can write

$$\begin{aligned} v_a =& f(v_O) \\ \approx& \frac{1}{2}a_2 v_E^2 + \left(K_a + \frac{3}{4}a_3 v_E^2\right) v_E \cos(\omega_0 t + \phi_0) \\ &+ \frac{1}{2}a_2 v_E^2 \cos 2(\omega_0 t + \phi_0) \\ &+ \frac{1}{4}a_3 v_E^3 \cos 3(\omega_0 t + \phi_0). \end{aligned} \tag{77}$$

This result allows us to identify the average large-signal amplification

$$K_{\mathrm{al}}(v_E) = K_a + \frac{3}{4}a_3 v_E^2 = K_a\left(1 - \alpha v_E^2\right) \tag{78}$$

where $\alpha = -(3a_3/4K_a)$ is a positive parameter ($a_3$ must be negative in order to model the gain compression when $v_E$ increases, a typical characteristic of what are known as *self-limiting oscillators*). We can also observe that $v_a$ shows a dc component as $v_E$ increases. Many implementations of the superregenerative receiver use this property to detect the oscillation envelope (for instance, by measuring the average current on a transistor) instead of including a separate envelope detector. One drawback of this technique is that an interfering component originated by the quench also appears in the dc component through $a_2$. By introducing the effect of quench, an analytical solution of (73) can be obtained when $K_{\mathrm{al}}$ exhibits separable variables

$$K_{\mathrm{al}}(t, v_E) = K_a(t)\left(1 - \alpha v_E^2\right). \tag{79}$$

This condition usually applies in practical circuits. For instance, BJT transistors exhibit an average large-signal transconductance (equivalent of $K_{\mathrm{al}}$), which is equal to the product of the small-signal transconductance $g_m$ (equivalent of $K_a$) and a nonlinear function of $v_E$ that can be approximated by a square law [26], [27]. The average large-signal damping function becomes

$$\zeta_l(t, v_E) = \zeta(t) + \alpha\left[\zeta_0 - \zeta(t)\right] v_E^2 \tag{80}$$

which, replaced in (73), yields the Bernoulli equation

$$\dot{v}_E + \zeta(t)\omega_0 v_E + \alpha\left[\zeta_0 - \zeta(t)\right]\omega_0 v_E^3 = 0. \tag{81}$$

Changing the variable

$$\begin{aligned} u =& v_E^{-2} \\ \dot{u} =& -2v_E^{-3}\dot{v}_E \end{aligned} \tag{82}$$

results in the linear differential equation

$$\dot{u}(t) - 2\zeta(t)\omega_0\, u(t) = 2\alpha\left[\zeta_0 - \zeta(t)\right]\omega_0. \tag{83}$$

The solutions of the homogeneous and the complete equations are, respectively,

$$\begin{aligned} u_h(t) =& U_0 e^{2\omega_0 \int_{t_b}^{t} \zeta(\lambda) d\lambda} = U_0 p^{-2}(t) \\ u_p(t) =& U_1(t) e^{2\omega_0 \int_{t_b}^{t} \zeta(\lambda) d\lambda} = U_1(t) p^{-2}(t) \end{aligned} \tag{84}$$

where

$$U_1(t) = 2\alpha\omega_0 \int_{t_b}^{t} \left[\zeta_0 - \zeta(\tau)\right] p^2(\tau) d\tau. \tag{85}$$

Undoing the change of variable yields

$$v_E(t) = \frac{1}{\sqrt{U_0 + U_1(t)}} p(t). \tag{86}$$

Finally, in order to obtain the constant $U_0$, we impose the condition that the function must agree with the small-signal envelope (linear mode), $v_E(t_1) = VK|H(\omega)|p(t_1)$, where $t_1$ is any instant after the sensitivity period in which the linear mode applies. Therefore, the expression for the envelope is

$$v_E(t) = \frac{1}{\sqrt{\left(\frac{1}{VK|H(\omega)|}\right)^2 + U(t)}} p(t) \tag{87}$$

where

$$U(t) = 2\alpha\omega_0 \int_{0}^{t} \left[\zeta_0 - \zeta(\tau)\right] p^2(\tau) d\tau. \tag{88}$$

The lower limit in the latter integral, $t_1$, has been replaced by zero, since $p^2(t)$ is small between $t = 0$ and $t = t_1$. From the previous result, we conclude the following.

1) $U(t)$ is a monotonic increasing function, since both $[\zeta_0 - \zeta(t)]$ and $p(t)$ are greater than or equal to zero. Granted that $p(t)$ is relatively narrow around $t = t_b$, the growth of $U(t)$ from its minimum to its maximum takes place near that instant.
2) The linear mode of operation takes place when the product $VK|H(\omega)|$ is small enough for $U(t)$ to be neglected at all times. In this case, (87) is reduced to that of the linear receiver.
3) The logarithmic mode takes place when $VK|H(\omega)|$ is large enough for $U(t)$ not to be neglected. This depends, in part, on the nonlinearity of the amplifier (parameter $\alpha$).

Fig. 7 plots the functions $\zeta(t)$, $U(t)$, and $v_E(t)$ of a typical superregenerative receiver operating under sinusoidal quench. The resulting envelope depends on the input amplitude $V$ at start-up. After the maximum is reached, the envelope is determined only by the damping function. When the peak gain $K$ is large enough, the envelope always reaches the limiting equilibrium amplitude: even in the absence of a signal, when it grows from noise.

### D. Area Under the Oscillation Envelope

Fig. 8 shows the build-up envelope in the logarithmic mode for two different initial conditions. For simplicity's sake, we will take the build-up curves to be truly exponential in form until

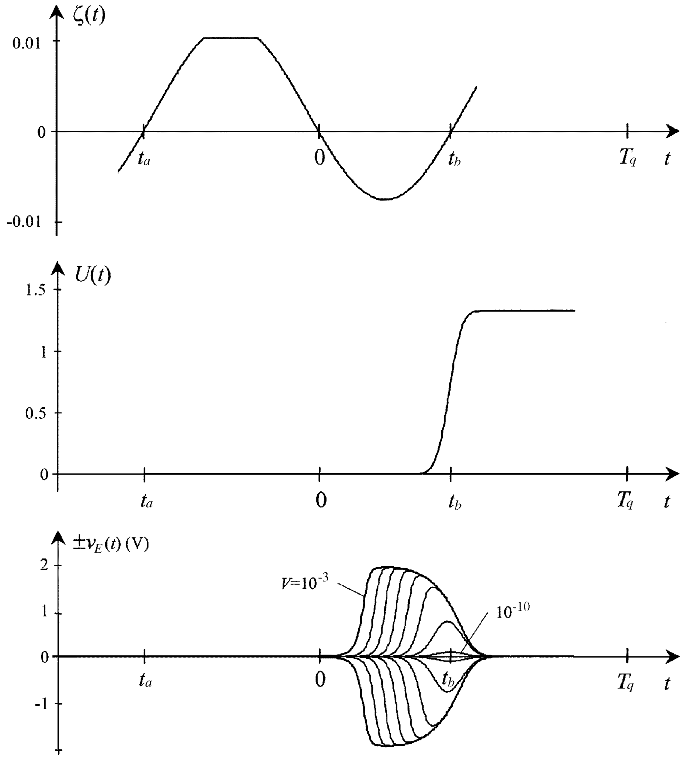


Fig. 7. Characteristic curves of the logarithmic mode of operation with sinusoidal quench.

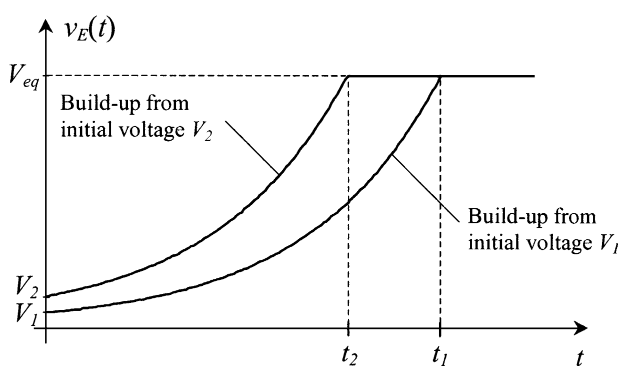


Fig. 8. Idealized envelopes of oscillation at build-up in the logarithmic mode.

they are suddenly limited at the equilibrium value $V_{\rm eq}$. In spite of this simplification, results are quite accurate in practice [2]. The limiting equilibrium amplitude can be expressed as

$$V_{\rm eq} = V_1 e^{\frac{t_1}{\tau_{\rm eq}}} = V_2 e^{\frac{t_2}{\tau_{\rm eq}}} \tag{89}$$

where $\tau_{\rm eq}$ is the equivalent time constant of build-up, so that

$$t_1 = \tau_{\rm eq} \ln \frac{V_{\rm eq}}{V_1}$$

and

$$t_2 = \tau_{\rm eq} \ln \frac{V_{\rm eq}}{V_2}. \tag{90}$$

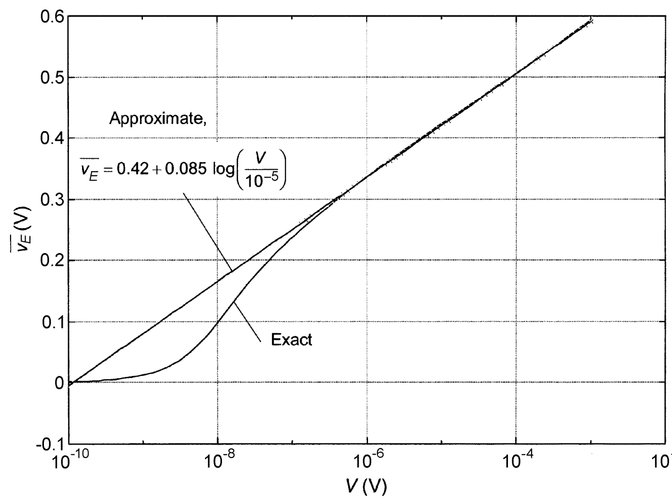


Fig. 9. Average of the envelope of the SRO output versus the input amplitude ($f_q = f_0/1000$, $K_0 = 0$ dB, $K_r K_s = 160$ dB, $\zeta_0 = 0.01 (Q_0 = 50)$, $\zeta_{\rm dc} = \zeta_0/5$, $\alpha = 0.1$, sinusoidal quench).

When the initial voltage changes from $V_1$ to $V_2$, the incremental area is

$$\begin{aligned}\Delta A &= V_2 \int_0^{t_2} e^{\frac{t}{\tau_{\rm eq}}} dt + V_{\rm eq}(t_2 - t_1) - V_1 \int_0^{t_1} e^{\frac{t}{\tau_{\rm eq}}} dt \\ &= \tau_{\rm eq} \left[ V_{\rm eq} \ln \left( \frac{V_2}{V_1} \right) - (V_2 - V_1) \right] \\ &\approx \tau_{\rm eq} V_{\rm eq} \ln \left( \frac{V_2}{V_1} \right) \end{aligned} \tag{91}$$

where it has been assumed that the initial values $V_1$ and $V_2$ are much smaller than the limiting voltage $V_{\rm eq}$. Assuming that $V_1 = V_{\rm ref} K$, where $V_{\rm ref}$ is a reference amplitude for which the total area under the envelope $A_{\rm ref}$ is known, the area for a generic amplitude $V_2 = VK$ is

$$A = A_{\rm ref} + \tau_{\rm eq} V_{\rm eq} \ln \left( \frac{V}{V_{\rm ref}} \right) \tag{92}$$

whereas the average of the envelope in the quench period is

$$\overline{v_E(t)} = \overline{v_{E\rm ref}(t)} + f_q \tau_{\rm eq} V_{\rm eq} \ln \left( \frac{V}{V_{\rm ref}} \right). \tag{93}$$

The logarithmic dependence, which is verified in Fig. 9 via simulation, entails low variations of the envelope average when large variations of the input amplitude take place, behaving as a sort of built-in automatic gain control. In particular, it can be demonstrated that, when AM with less than 100% modulation index is received, the demodulated output becomes independent of the input signal amplitude [10]. Notwithstanding this, distortion is unavoidably present.

## XI. Application Example: Design of a Conventional Superregenerative Receiver at 2.4 GHz

The architecture of a conventional superregenerative receiver is simply that of Fig. 1, in which the input signal is a narrowband amplitude modulation. Therefore, the desired component

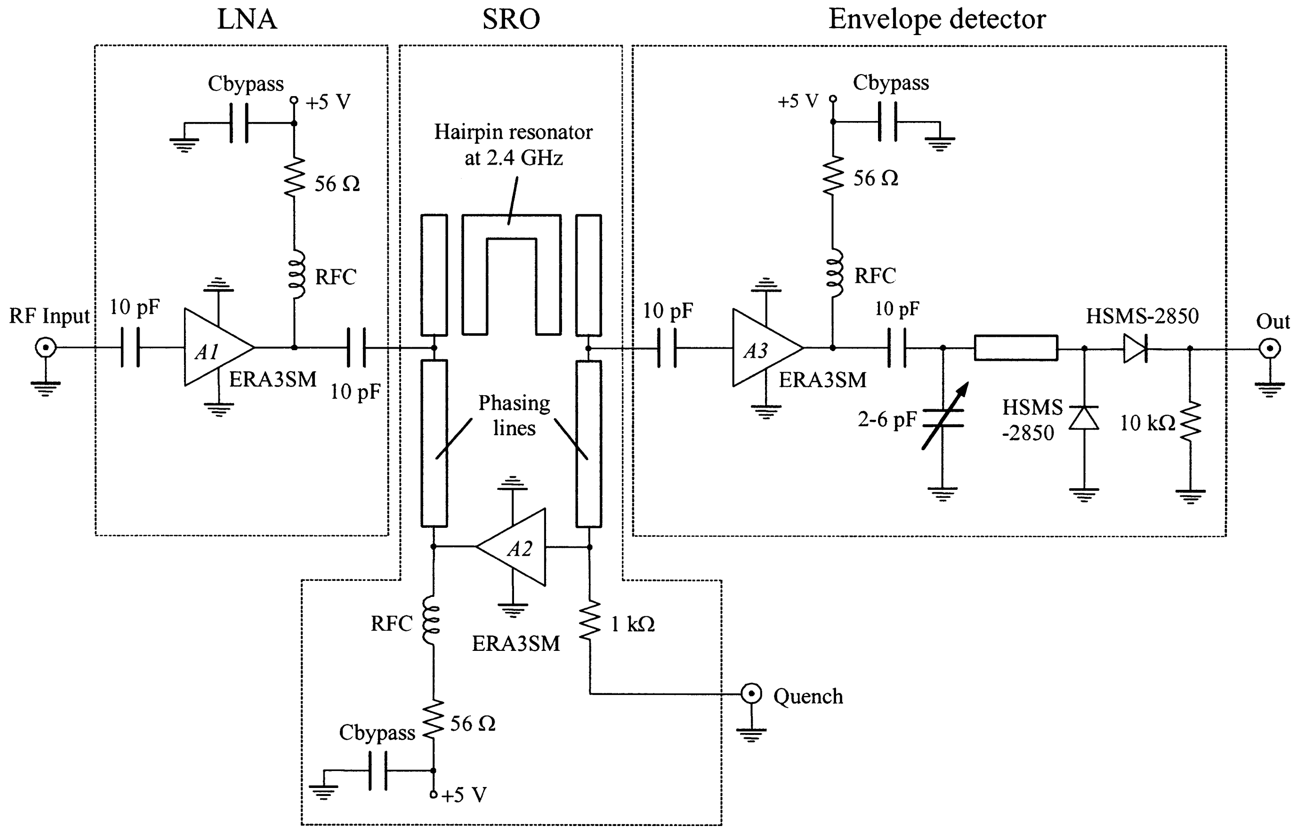


Fig. 10. Schematic of the RF part of the implemented receiver.

of the signal injected to the superregenerative oscillator can be expressed by

$$v(t) = V(t)\cos(\omega t + \phi) \tag{94}$$

where $V(t)$ is the amplitude containing the modulating information. We assume $p_c(t) = 1$ in this expression, which makes it extensible to any quench period. The narrow-band receiver samples the incoming signal asynchronously. In order to recover the information from the samples, the sampling frequency (equal to the quench frequency) must be at least twice the information bandwidth (Nyquist criterion). In practice, due to the limited selectivity of the low-pass filter, that rate must be higher, typically about ten times the information bandwidth. According to (57), the demodulated output can be approximated by

$$v_F(t) = V(t)K_{\text{eff}}\,|H(\omega)| \tag{95}$$

where the spectral components of $V(t)$ are assumed to be within the low-pass filter bandwidth.

Let us consider the design of a superregenerative receiver operating in the 2.4-GHz ISM band with the following specifications:

1) received modulation: ON–OFF keying (OOK), constant bit envelope;
2) bit rate: 100 kb/s;
3) peak amplitude at antenna output: 20 $\mu$V;
4) mode of operation: linear.

Fig. 10 shows the schematic of an implementation of the RF part of this receiver with monolithic amplifiers. $A1$ is the isolating input amplifier, with a gain of 18 dB, the SRO is built on $A2$, and $A3$ serves to complete the envelope detection. The SRO uses a feedback-oscillator configuration instead of the classical negative-resistance oscillator, in which the frequency-selective network is composed by a printed hairpin resonator coupled to two microstrip lines [28]. Note the evident parallelism of this circuit with the diagram in Fig. 1. This is a case in which we see the usefulness of thinking in terms of block diagram instead of particular *RLC* circuits. The loaded resonator provides a quiescent $Q$ equal to 50, a gain of $-8$ dB at resonance, and a phase shift of 165°. It can be shown that the results presented in this paper are extensible to the case in which the selective network introduces a phase shift, by including the corresponding value in (44). The measured phase shift of $A2$ at 2.4 GHz is 55° and, therefore, two additional microstrip lines have been included to achieve an overall loop shift, including the amplifier and the resonator, of 360°. The loop gain is controlled by the quench signal through the input of $A2$, which provides up to 18 dB, and the maximum quench frequency is about 8 MHz. The estimated maximum SRO output voltage under linear operation is 200 mV.

By taking ten times the modulation bandwidth (approximately 100 kHz), we have 1 MHz for the quench frequency. The chosen frequency must be as low as possible, since higher quench frequencies will provide a less selective receiver (a narrower sensitivity curve gives wider frequency response). The mean value of the damping function is set at one fifth of the quiescent value $\zeta_0$, which ensures negligible hangover. Assuming that linear operation is desired with the maximum output level of 200 mV, the SRO must provide a peak gain of 62 dB, which, added to the LNA gain, gives a total peak gain of 80 dB.

TABLE II
PARAMETERS CORRESPONDING TO THE SUPERREGENERATIVE RECEIVER IN THE APPLICATION EXAMPLE

| *Parameter* | *Symbol* | *Sinusoidal quench* | *Sawtooth quench* |
|---|---|---|---|
| Oscillation frequency | $f_0$ | 2.4 GHz | |
| Quench frequency | $f_q$ | 1 MHz | |
| Selective-network damping factor | $\zeta_0$ | 0.01 ($Q_0$=50) | |
| Average damping factor | $\zeta_{dc}$ | 0.002 ($Q_{dc}$=250) | |
| Hangover coefficient | $h$ | $7.5\times10^{-14}$ | |
| Peak-to-peak damping value | $\zeta_{pp}$ | 0.0072 | 0.0085 |
| Selective-network gain | $K_0$ | -8 dB | |
| Regenerative gain | $K_r$ | 27 dB | 31 dB |
| Superregenerative gain | $K_s$ | 43 dB | 39 dB |
| Normalized-envelope average | $\overline{p(t)}$ | -16 dB | -27 dB |
| Peak gain | $K$ | 62 dB | |
| Effective gain | $K_{eff}$ | 46 dB | 35 dB |
| -3 dB bandwidth | $\Delta f_{\text{-3dB}}$ | 4.1 MHz | 3.0 MHz |
| Overall quality factor | $Q$ | 587 | 789 |

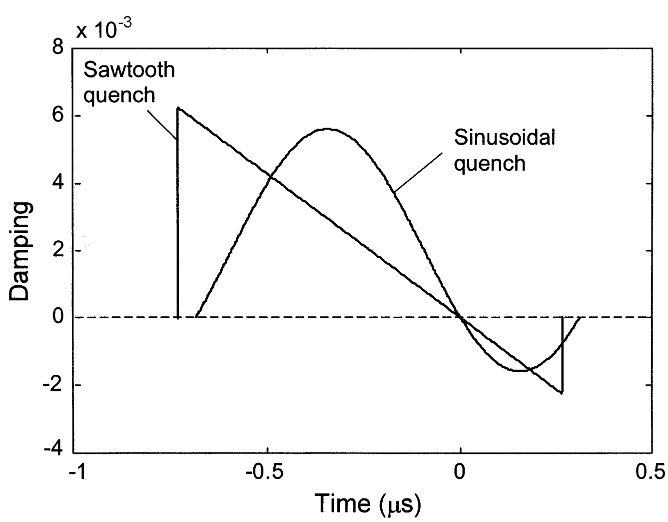


Fig. 11. Sinusoidal and sawtooth damping functions in the application example.

Simulation was carried out with the above constraints using the expressions in Table I for two common types of quench, sinusoidal and sawtooth. Integrals were computed numerically. The corresponding damping functions are presented in Fig. 11, and the resulting receiver parameters are included in Table II.

We can see from Table II that, although the peak gain applied by the SRO to the RF signal is 62 dB, the effective gains are only 46 and 35 dB, due to losses associated with the integration of the envelope. For instance, if the desired amplitude at the filter output is 200 mV, additional gains of 16 and 27 dB would be required, respectively, with an ideal envelope detector. The sawtooth quench provides a more selective curve at the price of lower gain. This is a typical tradeoff in superregenerative receivers.

As a result of the quench operation, the overall receiver $Q$ is about 650. It clearly improves the value of 50 provided by the selective network. This value, which is relatively high as a result of the moderate quench frequency, decreases as the quench frequency increases. For instance, at a quench frequency of 5 MHz, the $Q$ values are 145 for the sinusoidal and 216 for the sawtooth quench. We must emphasize that, in spite of the improved $Q$, the RF receiver bandwidth (about 3.5 MHz) is much greater than the modulation bandwidth (100 kHz). In other words, selectivity is far from that of an ideal receiver or, in practice, that of a superheterodyne receiver. This major inconvenience in narrow-band superregenerative receivers, nonetheless, turns out to be an advantage in spread-spectrum signal detection. In a spread-spectrum superregenerative receiver, the SRO is quenched synchronously with the received signal, taking a single sample per chip. In this way, the signal bandwidth and the receiver bandwidth become comparable [13].

Fig. 12 shows the signals measured on the implemented receiver with the OOK modulation and sinusoidal quench. The peak-to-peak voltage at the output of the envelope detector is 400 mV for an RF input level of $-87$ dBm (peak envelope power equal to $-84$ dBm). The experimental verification of all the parameters and functions presented in this paper is not easy, as in most cases it requires complex procedures. This is especially true at the frequency of 2.4 GHz. Therefore, the results presented here are limited to items that are relatively easy to measure and observe: namely, the selectivity of the receiver and the envelope of the pulses generated in the SRO. Fig. 13 shows the selectivity curves measured from the out-of-band signal rejection. With sinusoidal quench, the receiver can be adjusted to provide a $-3$-dB bandwidth of 4.1 MHz, according to Table II. When operated with sawtooth quench, the bandwidth is reduced to 3.3 MHz, 10% above the predicted value of 3 MHz. Far from the reception center frequency, a noteworthy difference between measurements and predictions is observed. This behavior is systematically observed in superregenerative receivers [19]. Fig. 14 shows the envelope of the pulses generated in the SRO. With

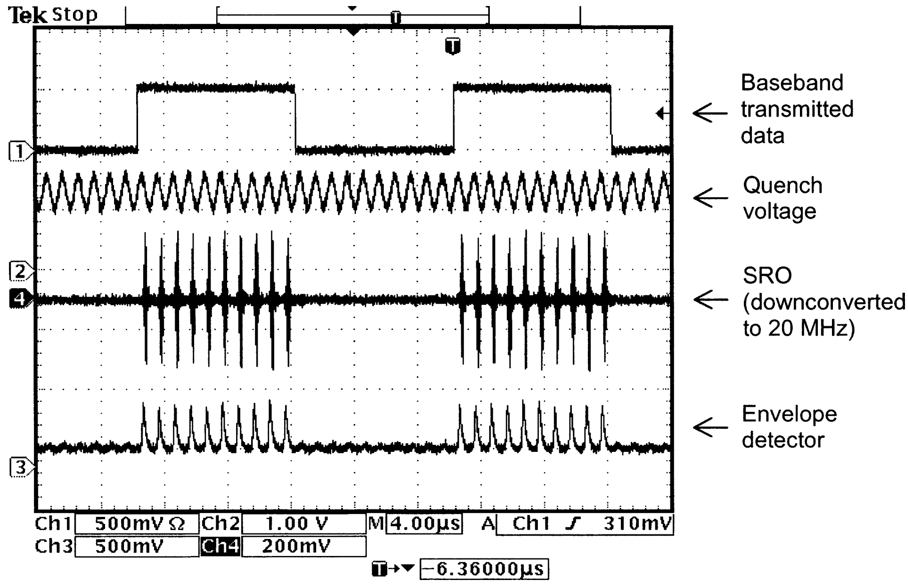


Fig. 12. Measured signals in the implemented receiver.

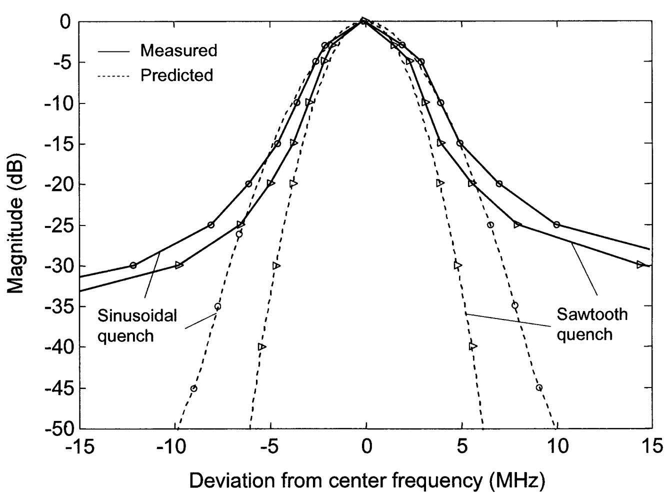


Fig. 13. Frequency response of the implemented receiver.

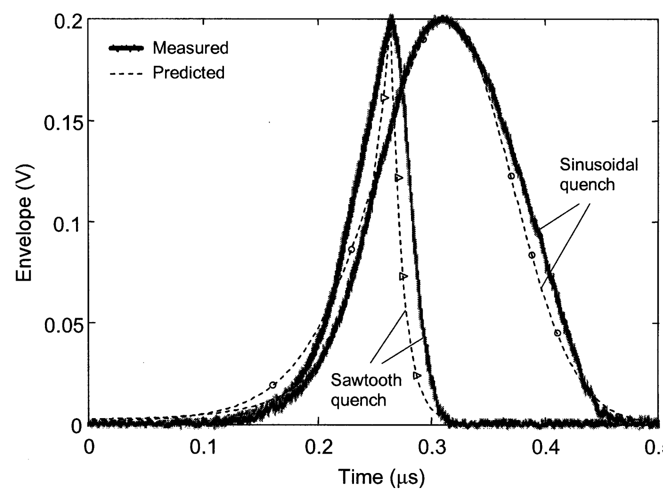


Fig. 14. Envelope of the oscillation generated in the SRO in the linear mode.

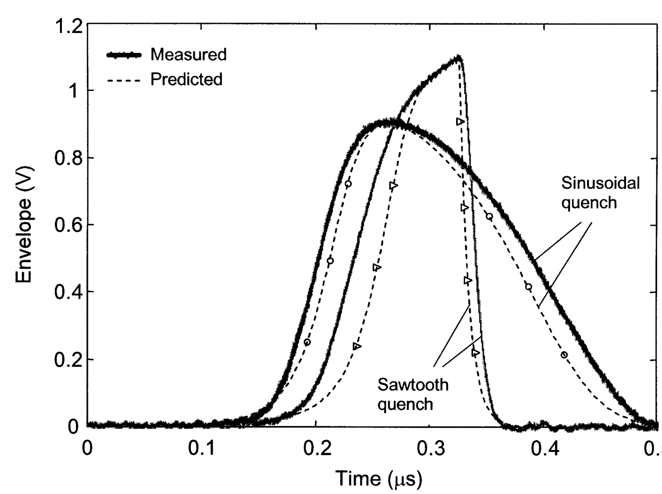


Fig. 15. Envelope of the oscillation generated in the SRO in the logarithmic mode.

sinusoidal quench, the measurements agree very well with the predictions. In the case of sawtooth quench, the measured pulse is considerably larger than the predicted one. This effect occurs because the circuit smoothes the abrupt transitions in the quench voltage.

As a final experiment, a gain increase of 40 dB was applied to the receiver in order to operate in the logarithmic mode. The measured oscillation envelopes are shown in Fig. 15. For the predicted envelopes, the parameter $\alpha$ in (79) was set equal to 0.2. It was chosen to provide the same peak amplitude as the measures. The fact that the shapes as predicted and measured exhibit great similarity validates the solutions presented for this mode of operation.

## XII. Conclusion

We have presented a novel and unified approach to the theory of superregenerative receivers based on their generic block diagram. The study applies to a wide class of superregenerative oscillators, including negative resistance and feedback oscillators, and shows that, in any case, high gain and tuning capability can be achieved from a single active device. Meaningful normalized parameters and functions have been defined and generic analytic expressions have been provided for both the linear and the logarithmic modes of operation. It can be remarked that, in particular, the shape of the input signal envelope and the sensitivity curve play an important role in receiver gain and selectivity. Finally, we have shown how the presented approach can be applied to the design of a practical superregenerative receiver.

## Appendix
## Frequency Response in the Sinusoidal Steady State With Appreciable Hangover

The frequency response of a superregenerative receiver operating in the sinusoidal steady state with appreciable hangover can be calculated as follows. The excitation

$$v(t) = V\cos(\omega t + \phi) \tag{96}$$

must be broken down into the superposition of pulses matching each quench period

$$v(t) = V\sum_{m=-\infty}^{\infty} p_c(t - mT_q)\cos\left(\omega(t - mT_q) + m\omega T_q + \phi\right) \tag{97}$$

where $p_c(t)$ is a rectangular pulse allocated in a single quench period. By applying superposition, the response of the receiver results in

$$\begin{aligned} v_O(t) = VK\,|H(\omega)|\sum_{m=-\infty}^{\infty} p(t - mT_q) \\ \times\cos\left(\omega_0 t + m(\omega-\omega_0)T_q + \phi + \angle H(\omega)\right) \end{aligned} \tag{98}$$

which can be evaluated through the fasor sum

$$\begin{aligned} \overline{V_O}(t) &= VK\,|H(\omega)|\sum_{m=-\infty}^{\infty} p(t - mT_q) \\ &\quad\times e^{j\left(\omega_0 t + m(\omega-\omega_0)T_q + \phi + \angle H(\omega)\right)} \\ &= VKH(\omega)e^{j(\omega_0 t + \phi)}\sum_{m=-\infty}^{\infty} p(t - mT_q) \\ &\quad\times e^{jm(\omega-\omega_0)T_q}. \end{aligned} \tag{99}$$

For the sake of simplicity, we will evaluate this expression *at the end* of the quench period, when the oscillation amplitude achieves its maximum, i.e., at $t = t_b$. Using the expression for the normalized output envelope

$$p(t) = \begin{cases} e^{-\omega_0\int_{t_b}^{t}\zeta(\lambda)d\lambda}, & t > 0 \\ 0, & \text{otherwise} \end{cases} \tag{100}$$

it is possible to express

$$\begin{aligned} &p(t_b - mT_q) \\ &= \begin{cases} e^{-\omega_0\int_{t_b}^{t_b - mT_q}\zeta(\lambda)d\lambda} = e^{m\zeta_{dc}\omega_0 T_q}, & m \le 0 \\ 0, & \text{otherwise.} \end{cases} \end{aligned} \tag{101}$$

Consequently, as $\zeta_{dc} > 0$, the sum results in

$$\begin{aligned} \overline{V_O}(t_b) &= VKH(\omega)e^{j(\omega_0 t_b + \phi)}\sum_{m=0}^{\infty} e^{-m(\zeta_{dc}\omega_0 + j(\omega-\omega_0))T_q} \\ &= VKH(\omega)e^{j(\omega_0 t_b + \phi)}\frac{1}{1 - e^{-(\zeta_{dc}\omega_0 + j(\omega-\omega_0))T_q}} \end{aligned} \tag{102}$$

revealing that the additional factor

$$F(\omega) = \frac{1}{1 - e^{-(\zeta_{dc}\omega_0 + j(\omega-\omega_0))T_q}} \tag{103}$$

must be included in the frequency response of the receiver. By introducing the hangover coefficient (52)

$$h = e^{-\zeta_{dc}\omega_0 T_q} \tag{104}$$

it is possible to rewrite (103) as

$$F(\omega) = \frac{1}{1 - he^{-j(\omega-\omega_0)T_q}}. \tag{105}$$

The modulus of this function

$$\begin{aligned} |F(\omega)| &= \frac{1}{\left|1 - he^{-j(\omega-\omega_0)T_q}\right|} \\ &= \frac{1}{\sqrt{1 + h^2 - 2h\cos(\omega-\omega_0)T_q}} \\ &= \frac{1}{\sqrt{1 + h^2 - 2h\cos 2\pi\frac{f - f_0}{f_q}}} \end{aligned} \tag{106}$$

is a periodic function showing the extreme values

$$\begin{aligned} |F(\omega)|_{\max} &= \frac{1}{1-h}, \quad f = f_0 + kf_q \\ |F(\omega)|_{\min} &= \frac{1}{1+h}, \quad f = f_0 + (2k+1)\frac{f_q}{2}. \end{aligned} \tag{107}$$

## References


[1] E. H. Armstrong, “Some recent developments of regenerative circuits,” in *Proc. IRE*, vol. 10, Aug. 1922, pp. 244–260.
[2] J. R. Whitehead, *Super-Regenerative Receivers*. Cambridge, U.K.: Cambridge Univ. Press, 1950.
[3] F. G. Stremler, “Design of a small radar altimeter for balloon payloads,” in *3rd Int. Geosci. Electron. Symp. Dig. Tech. Papers*, New York, 1971, p. 1.
[4] C. J. Milner and G. S. Shell, “A super-regenerative microwave Doppler moving-target indicator,” *IEEE Trans. Veh. Technol.*, vol. VT-17, pp. 13–23, Oct. 1968.
[5] W. G. McCoy, “Design of a superregenerative receiver for solar powered applications,” *IEEE Trans. Consum. Electron.*, vol. 38, pp. 869–873, Nov. 1992.
[6] L. N. Deryugin, B. P. Kulakov, and V. K. Nurmukhametov, “Superregenerative amplification possibilities in a Q-switched laser,” *Radio Eng. Electron. Phys.*, vol. 16, no. 1, pp. 119–126, Jan. 1971.
[7] F. X. Moncunill Geniz and J. M. M. López, “Receptor superregenerativo para comunicaciones ópticas no guiadas,” M.S. Thesis, Univ. Politècnica de Catalunya, Barcelona, Spain, 1992.
[8] M. C. España-Boquera and A. Puerta-Notario, “Bit-error rate and frequency response in superregenerative semiconductor laser receivers,” *Opt. Lett.*, vol. 24, no. 3, pp. 157–159, Feb. 1999.
[9] I. Hickman, *Practical RF Handbook*, 2nd ed. Oxford, U.K.: Newnes, 1997.

[10] R. Feick, O. Rojas, and A. Mackay, "Modeling and simulation of the superregenerative receiver," *IEEE Trans. Consum. Electron.*, vol. 43, pp. 92–102, May 1997.
[11] F. X. Moncunill, O. Mas, and P. Palà, "A direct-sequence spread-spectrum super-regenerative receiver," in *Proc. ISCAS*, vol. I, 2000, pp. 68–71.
[12] F. X. Moncunill-Geniz, O. Mas-Casals, and P. Palà-Schönwälder, "A comparative analysis of direct-sequence spread-spectrum super-regenerative architectures," in *Proc. ISCAS*, vol. IV, 2001, pp. 120–123.
[13] F. X. Moncunill Geniz, P. Palà-Schönwälder, and O. Mas-Casals, "New super-regenerative architectures for direct-sequence spread-spectrum communications," Ph.D. dissertation, Univ. Politècnica de Catalunya, Barcelona, Spain, 2002.
[14] L. Hernandez and S. Paton, "A superregenerative receiver for phase and frequency modulated carriers," in *Proc. ISCAS*, vol. 3, 2002, pp. 81–84.
[15] T. E. McEwan, "Micropower RF transponder with superregenerative receiver and RF receiver with sampling mixer," U.S. Patent 5 630 216, May 13, 1997.
[16] G. Mapes, "Superregenerative oscillator RF receiver with differential output," U.S. Patent 20 020 168 957, Nov. 14, 2002.
[17] V. Leibman, "Superregenerative low-power receiver," W.O. Patent 03 009 482, Jan. 30, 2003.
[18] A. Hazeltine, D. Richman, and B. D. Loughlin, "Superregenerator design," *Electronics*, vol. 21, pp. 99–102, Sep. 1948.
[19] A. Vouilloz, M. Declercq, and C. Dehollain, "A low-power CMOS super-regenerative receiver at 1 GHz," *IEEE J. Solid-State Circuits*, vol. 36, pp. 440–451, Mar. 2001.
[20] R. Grimshaw, *Nonlinear Ordinary Differential Equations*. Boca Raton, FL: CRC Press, 1993.
[21] M. Braun, *Differential Equations and Their Applications*, 3rd ed. New York: Springer-Verlag, 1986.
[22] F. X. Moncunill-Geniz, O. Mas-Casals, and P. Palà-Schönwälder. Demodulation capabilities of a DSSS super-regenerative receiver. presented at 2nd Online Symp. Electron. Engineers (OSEE). [Online] Available: http://www.techonline.com/community/20214
[23] W. E. Bradley, "Superregenerative detection theory," *Electron.*, vol. 21, pp. 96–98, Sep. 1948.
[24] H. A. Glucksman, "Superregeneration—an analysis of the linear mode," in *Proc. IRE*, vol. 37, May 1949, pp. 500–504.
[25] A. Vouilloz, "Récepteur micropuissance à super-réaction intégré en technologie CMOS," Ph.D. dissertation, École Polytechnique Fédérale de Lausanne, Lausanne, Switzerland, 2002.
[26] K. Clarke and D. Hess, *Communication Circuits: Analysis and Design*. Brooklyn, NY: Addison-Wesley, 1971.
[27] D. Pederson and K. Mayaram, *Analog Integrated Circuits for Communication*. Norwell, MA: Kluwer, 1991.
[28] D. M. Pozar, *Microwave Engineering*. New York: Wiley, 1998.

**F. Xavier Moncunill-Geniz** received the Engineer of Telecommunication and Ph.D. degrees from the Universitat Politècnica de Catalunya, Barcelona, Spain, in 1992 and 2002, respectively.

He is currently an Assistant Professor with the Departament de Teoria del Senyal i Comunicacions, Escola Tècnica Superior d'Enginyeria de Telecomunicació de Barcelona, Spain, in the field of circuit theory and analog electronics. His main research area is RF circuit design, with particular emphasis on the theory and implementation of new architectures of superregenerative receivers.

**Pere Palà-Schönwälder** (S'89–A'95) received the Engineer of Telecommunication and Ph.D. degrees from the Universitat Politècnica de Catalunya, Barcelona, Spain, in 1989 and 1994, respectively.

He is currently an Associate Professor with the Departament de Teoria del Senyal i Comunicacions, Escola Universitària Politècnica de Manresa, Spain. He has been the manager of several Spanish research projects. His research interests include computer-aided circuit design, nonlinear circuits, and RF communication electronics.

**Orestes Mas-Casals** received the Engineer of Telecommunication and the Ph.D. degrees from the Universitat Politècnica de Catalunya, Barcelona, Spain, in 1990 and 1997, respectively.

He is currently an Associate Professor with the Departament de Teoria del Senyal i Comunicacions, Escola Tècnica Superior d'Enginyeria de Telecomunicació de Barcelona, Spain, where he teaches circuit theory and analog electronics. His research interests include fuzzy systems, control theory, and the development of free software applications in those fields.